buildings

MDPI

Article

Evaluation Model of Distributed Photovoltaic Utilization in Urban Built-Up Area

Siyuan Chen [1,2], Zao Zhang [1,*], Cheng Wang [3,*], Lifeng Tan [4], Huanjie Liu [1], Hong Yuan [1], Rui Zhang [1] and Rui Hu [1]

[1] School of Architecture, Tianjin University, Tianjin 300384, China; liuhuanjie_arch@163.com (H.L.)
[2] China Northeast Architectural Design & Research Institute Co., Ltd., Shenzhen 518057, China
[3] School of Art, Tianjin Chengjian University, Tianjin 300384, China
[4] School of Architecture, Tianjin Chengjian University, Tianjin 300072, China; tanlf_arch@163.com
* Correspondence: zao.zhang@tju.edu.cn (Z.Z.); cheng_gsa@163.com (C.W.)

Abstract: Photovoltaic (PV) power generation is emerging as a key aspect of the global shift towards a more sustainable energy mix. Nevertheless, existing assessment models predominantly concentrate on predicting the overall capacity of PV power generation, often neglecting temporal dynamics. Drawing upon the urban energy substitution rate, utilization rate, and power supply stability, this study has devised a comprehensive evaluation model for the utilization of distributed photovoltaic systems (SUS). This model integrates the quantification of spatio-temporal features inherent in urban settings and buildings. Using Hohhot city as a case study, this study conducted simulations to analyze how the installation of PV systems affects the electricity consumption patterns across different land plots within the urban core. The study additionally examines how urban planning influences the adoption of PV power, taking into account both the timing of PV power usage and the stage of PV technology development. The evaluation model surpasses the constraints of current urban PV assessments, which primarily emphasize enhancing power generation potential without adequately quantifying supply–demand dynamics or spatial and temporal variations. This breakthrough significantly improves the precision and reliability of assessing the efficiency of distributed PV systems. Its implications extend widely to subsequent comprehensive evaluations of urban PV applications.

Keywords: distributed photovoltaic; evaluation model; sustainable energy; quantitative analysis

Citation: Chen, S.; Zhang, Z.; Wang, C.; Tan, L.; Liu, H.; Yuan, H.; Zhang, R.; Hu, R. Evaluation Model of Distributed Photovoltaic Utilization in Urban Built-Up Area. *Buildings* **2024**, *14*, 943. https://doi.org/10.3390/buildings14040943

Academic Editor: Constantinos A. Balaras

Received: 18 February 2024
Revised: 22 March 2024
Accepted: 26 March 2024
Published: 29 March 2024

1. Introduction

Today, 80% of the world's GDP comes from 2% of the world's cities, but they consume nearly 75% of the world's resources [1]. Renewable energy has become a crucial issue that must be addressed in the national development process, as energy security is directly linked to economic growth [2,3].

As of 2018, the total global installed PV capacity has grown to 480 GW (from only 1 MW in 1979), accounting for approximately 2% of global energy consumption [4]. This demonstrates a rapid development trend. In the future, until 2050, PV power generation will continue to drive the structural transformation of renewable energy worldwide due to its abundant resource availability, substantial market potential, and cost competitiveness [5]. One of the most important forms of photovoltaic power generation is distributed photovoltaic power generation, which involves installing photovoltaic modules on the surfaces of buildings in cities to generate electricity [6].

However, regarding distributed photovoltaics in urban built-up areas, energy spatial planning and urban planning will both play crucial limiting roles [7]. The current indicators focus on enhancing the production potential of generation, but there are significant shortcomings in considering the energy supply-and-demand relationship, as well as spatial and temporal variations.

In the past, the assessment of urban PV potential focused on the installable area for PV systems and the power generation capacity in different urban areas. Firstly, evaluation

indicators should be established. At present, several common evaluation indicators or standards are shown in Table 1. However, the established research indicators are relatively single, only consider the total amount of power generation/total amount of power consumption, ignoring the temporal sequence of PV power consumption and the stage of development.

Table 1. Main application indicators of current urban PV potential assessment work.

Indicators	Definition of Indicator	Index Source
PV area per capita	Area PV available roof area/area total population	IEA-PVPS [8]
Per capita installed PV capacity	Total installed PV capacity/total population of the region	Izquierdo, S. [9]
$SAFAR_n$	Photovoltaic available area on building exterior surface/building area	Jouri, K. [10]
Photovoltaic permeability	Regional total installed PV capacity/regional peak load	Zhao, B., Xiao, C.H., et al. [11]
PV cost/PV utilization	Regional photovoltaic installation cost and electricity sales revenue by weight comprehensive comparison	Cheng, M., Zhao, S.H., et al. [12]
Solar energy grading factor	Area available for photovoltaic power generation/area of land use	Sigrid Lindner of Ecofys [13]
RPVID	Area of photovoltaic available on the regional roof/area of land use	Zhang, H. [14]

In addition to the relevant indicators, the methodology for potential assessment is at the core of the research. The urban PV potential is usually assessed by giving a percentage of the building surface that is suitable for urban PV development (usually the roof utilization factor). In terms of the scope of the assessment, calculations are conducted for specific building types. For instance, Enongene et al. analyzed and modeled typical buildings to calculate the PV potential of urban areas in Nigeria [15]. There are also projections on a national scale. For example, Rosas-Flores et al. assessed the energy potential of Mexican city pools and rural households through large-scale grid-connected and interconnected PV systems [16]. Bodis et al. assessed the potential PV power generation for the entire European Union, estimating 680 TWh per year [17]. In terms of assessment calculation methods, accurate quantitative studies incorporating GIS systems have also been used by an increasing number of scholars for assessing urban PV potential [18–21]. Alaa Alhamwi et al. proposed the establishment of a GIS open-source platform for optimizing urban distributed energy systems [22]. Mariela Tapia et al. utilized GIS and associated building feature extraction algorithms to evaluate rooftop solar PV potential in various cities in Ecuador [23]. Jiang Liu et al. combined 3D building data with GIS to accurately assess the solar PV potential of rural roofs and facades [24]. Most of these potential assessment studies focus on a city scale or specific building types to maintain the high accuracy provided by the aforementioned methods. There are also uncertain predictions for intricate cities, such as the study by Diana Bernasconi and Giorgio Guariso on surface quantities and the potential of rooftop PV in complex cities. This study utilized morphological clustering methods instead of relying on remote sensing data for large-scale studies [25].

Most of the previous studies on PV potential have focused on estimating the capacity of PV power generation by predicting the ratio of PV power production to the current urban electricity consumption. However, the discussion focusing on the theoretical increase in the total power generated has also contributed to overly optimistic expectations. On the one hand, PV power output is greatly influenced by environmental factors. Without considering the impact of specific climatic conditions such as clouds and rain, PV power output typically peaks at midday and follows a clear normal distribution. As the primary source of urban energy consumption, the pattern of electricity load change is associated with users' behavioral characteristics and exhibits variations based on the diverse functions of buildings. The two do not always show a similar trend of change due to the simultaneity

of power output and consumption behavior. The excess PV power output cannot be effectively consumed immediately.

The primary solution to this problem is to depend on different energy storage technologies to maintain the balance between system supply and demand, thereby enhancing its overall stability. However, due to cost constraints, energy storage facilities cannot be widely used for commercial purposes in urban areas. This creates a significant technological bottleneck that hinders the utilization of photovoltaics [26]. The excess PV power can be transferred to other urban areas through grid-connected methods. However, in the future, when the city relies on PV energy as the primary source of electricity, the excess power cannot be transferred and consumed within the city. Therefore, it is necessary to propose a dynamic indicator to introduce the concept of PV consumption timing. This indicator, known as the PV Utilization Assessment Method (SUS), is based on the energy substitution rate, PV utilization rate, and PV utilization stability. It aims to comprehensively reflect the current status of PV application and integration in all regions of the city.

2. Materials and Methods

2.1. Research Materials

In the research of distributed PV in urban built-up areas, we selected the central city of Hohhot as the primary research object (Figure 1). Hohhot is classified as a second-tier region for solar energy sunshine resources in China, indicating better potential for PV development. It is considered a priority region for large-scale PV installations in the future. At the same time, Hohhot's three types of industrial structure ratios are very similar to those of China, and its urban function ratio can reflect the characteristics of China's urban economic development.

Figure 1. Location of the study area. (The map of China (left) was provided by Ministry of Natural Resources of China (Approval number: GS(2019)1673)).

Hohhot city in Inner Mongolia is located between 110°46′–112°10′ E and 40°51′–41°8′ N. It belongs to the primary solar resource distribution area of China. The total annual solar radiation is 6241.19 MJ/m^2 (about 1734 kWh/m^2), and the effective sunshine time is 2599.7 h. This indicates promising prospects for PV development. Meanwhile, in terms of electricity consumption load in Hohhot, the total area of various types of construction land reached 329,554,000 square meters. The entire society in Hohhot used 33,084,270,000 kWh

of electricity in 2022. The city mentioned above has a high electricity demand, coupled with abundant sunshine energy, that holds great potential for development [27].

The information on the urban built-up area of Hohhot was obtained from the planning data and relevant policies and regulations of the relevant departments. The building load information was calculated and summarized based on the meter readings provided by the state power department. In addition, all relevant data, including the comparison of photovoltaic technology characteristics, the land-cover status of centralized photovoltaic land, the data on protected areas and global sunshine radiation, the distribution of population density, per capita electricity consumption, meteorological data, and other information, were sourced from open data provided by countries and various global organizations.

2.2. Research Methods

2.2.1. Formulate SUS PV Potential Assessment Indicators

Energy Substitution Rate

The concept of energy substitution rate (ESR) considers the time sequence and actual situation of photovoltaic electricity consumption to reflect the degree of substitution of renewable energy for traditional electricity consumption. It measures the degree of spontaneous self-use after the integrated application of photovoltaic systems in various urban areas. Specifically, it can be divided into the overall energy substitution rate (ESR) and the hourly energy substitution rate (ESR_i) of regional plots, as shown in Equations (1) and (2).

The hourly energy substitution rate (ESR_i) is as follows:

$$ESR_i = \frac{Pe_i}{Load_i} \quad (1)$$

The overall energy substitution rate (ESR) is as follows:

$$ESR = \frac{\sum_i^n Pe_i}{\sum_i^n Load_i} \quad (2)$$

ESR_i is the hourly energy substitution rate of a block area in the city at the ith time. ESR is the overall energy substitution rate in the period from 0 to 23 points in a certain area of the city. Pe_i (kWh) is the consumption of photovoltaic power produced by a block in a city at the ith time. $Load_i$ (kWh) is the electricity consumption load at the ith moment of a block in a city. PV_i (kWh) is the photovoltaic power generation at the ith moment of a block in a city.

Photovoltaic Utilization Rate (PUR)

In addition to considering the replacement degree of traditional energy sources, the daily load curve patterns in various urban areas will change according to the different building functions (residential, office, commercial, etc.). In this paper, the photovoltaic utilization rate [28] (PUR, PV utilization ratio) is a supplement to the PV utilization ratio index (ESR), which is defined as the ratio of actual available photovoltaic power generation to the maximum allowable power generation under theoretical conditions within a specific operating period.

$$PUR = \frac{\sum_i^n Pe_i}{C \cdot T} \quad (3)$$

PUR is the photovoltaic utilization rate of a certain area in the city. C (kWh) is the installed photovoltaic capacity of a certain area in the city. T (h) is the theoretical working hours of PV module in a certain area of the city.

Standard Deviation of Hourly Replacement Rate

Photovoltaic power generation technology is significantly influenced by climate change factors. The stability of power supply output exhibits considerable volatility with changes in weather and time. This instability is evident in the variation of the photovoltaic

daily hourly replacement rate (ESR_i) over time. In this study, the standard deviation (Stdev) of the hourly PV replacement rate was used to reflect the power supply stability of each urban parcel after PV application, as shown in Formula (4):

$$\text{Stdev} = \sqrt{\frac{1}{n} \cdot \sum_{i}^{n} (ESR_i - R_i)^2} \quad (4)$$

Stdev is the standard deviation of the hourly PV replacement rate. R_i is the arithmetic average of daily hourly PV replacement rate. n is the number of power generation hours during the photovoltaic available period of the plot.

2.2.2. SUS PV Potential Assessment Model

The PV potential assessment of SUS mainly includes four steps: basic data collection, data processing, SUS index, and formulation of regional planning and adjustment strategies.

The basic data collection part includes load information data such as, daily load rate curves of various buildings and their peak load densities; urban model information data such as, the building floor area ratio, building density, and functional ratio of each building; and meteorological information data such as, annual sunshine hours and annual hourly sunshine radiation intensity.

Firstly, the corresponding hourly load and hourly power generation of each block are calculated. Based on this data, the ESR, PUR, and Stdev indexes of each block are calculated, respectively.

Finally, through the classification and analysis of the three indicators, the priority of photovoltaic development in each region is evaluated. In this way, it can be determined which land parcel's functional form is more suitable for the future energy structure transformation. Then, the location layout and urban planning can be adjusted for the unfavorable areas of photovoltaic development to optimize the overall utilization of photovoltaics in the city (Figure 2).

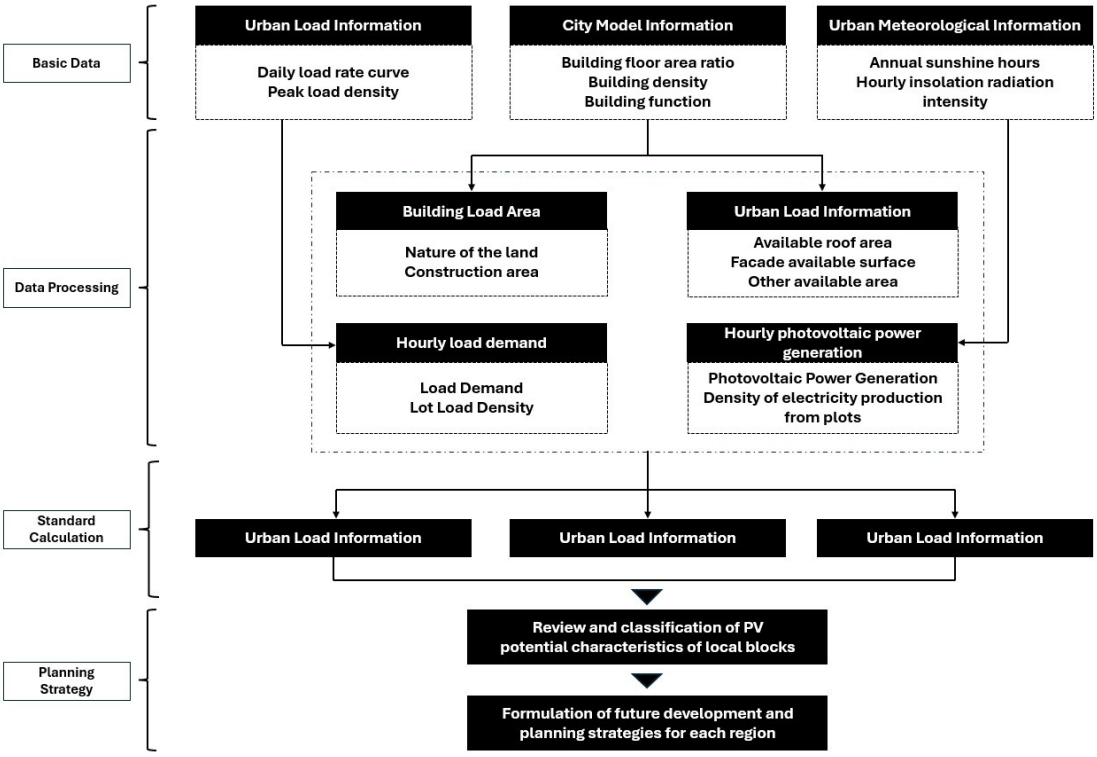

Figure 2. Framework diagram of SUS PV potential assessment procedure. Source: Drawn by the author.

2.2.3. Urban Basic Form Calculation

Based on the overall urban plan and zoning regulations of Hohhot City for 2020–2030, this paper examines the three indices of building function, building density, and floor area ratio for each block within the designated planning area.

Building Volume Rate for a Certain Area

The basic data was provided by the Hohhot Urban and Rural Planning and Design Institute. The overall plan (2020–2030) includes vector information such as land use boundaries, land use characteristics, and road network planning for various areas. The zoning plan includes Huhhot Hui District, Saihan District, Xincheng District, and Yuquan District. The controlled range of land use intensity (plot ratio) is as follows: A plot ratio >4.5, B plot ratio 3.5–4.5, C plot ratio 2.0–3.4, and D plot ratio <2.0 (Figure 3).

Figure 3. Plot ratio simulation results of each block. Source: Drawn by the author. Building density of a certain area.

Building density (BD) refers to the ratio between the total base area of a building and the land area of a plot within a certain range. It is an important indicator that reflects the building form information of different blocks. Since it is still in the planning stage, this paper adopts a calculation method for building density based on the characteristics of a typical urban plot layout. The building density of each block can be roughly calculated by Equation (5):

$$BD' = (1 - G - R - S - P) \times 100\% \quad (5)$$

BD′ means the preliminary estimated building density of a certain block. G is the green land rate of a place. R is the land use rate of a block of roads. S is the rate of supporting public construction land for a residential parcel. P is the percentage of ground parking land in a certain area.

Draw up the Number of Building Floors and Adjust Building Density

According to Equations (4) and (5), the building density (BD′) of each block can be preliminarily estimated. At the same time, according to the relationship between floor area

ratio and building density, the average floor number (F′) of each block building can be further calculated. To facilitate further prediction and analysis, we assume that buildings in each given land parcel have the same number of building floors and in turn adjust the preliminary calculated building density (BD′) results for each parcel. Finally, the proposed building density (BD) and the number of building floors (F) of each block can be used for calculation. The calculation process is shown in Equations (6)–(8).

$$f' = \frac{FAR}{BD'} \tag{6}$$

$$f = \text{roundup}(f' + 0.5) \tag{7}$$

$$BD = \frac{FAR}{f} \tag{8}$$

FAR is the volume ratio of a certain area. F′ means the average number of building floors preliminarily calculated for a certain block. BD′ is the building density preliminarily calculated for a certain block. f is the proposed number of building floors after adjustment of a certain block and is the result of f′ rounded up. BD is the proposed building density after the adjustment of a place block.

2.2.4. Calculation of Available PV Area

Available Rooftop PV Area

The rooftops of various buildings in the city are the primary locations for photovoltaic applications. For specific buildings, the available roof area can be determined through software simulation or manual screening. However, for a large range of urban areas, it is usually calculated by the rooftop photovoltaic utilization coefficient (Kr). The roof utilization coefficient refers to the research results of Zhang Hua in 2017 (Table 2). The available area of rooftop PV (Sr) of each building block can be calculated by Equation (9).

$$Sr = BD \times A \times Kr \tag{9}$$

Sr (m^2) is the available rooftop photovoltaic area of a block building. A (m^2) is the land area of a certain place. Kr is the rooftop photovoltaic utilization coefficient corresponding to a block type.

Table 2. PV roof utilization factor at a glance and the values taken in this paper [29].

Land Use Category		City Discount Rate	Neighborhood Discount Rate	Monomeric Discount Rate	Rooftop PV Utilization Factor (Kr)	Mean Value (Kr) Values
Residential buildings	Low-rise residential area	1	1	0.3–0.5	0.3–0.5	0.4
	Multi-story residential area	0.85–1	0.95–0.98	0.55–0.7	0.44–0.69	0.57
	High-rise residential area	0.9–1	0.7–0.95	0.4–0.6	0.25–0.57	0.41
Multi-story public buildings		1	1	0.7–0.85	0.7–0.85	0.78
High-rise public buildings		0.85–1	0.51–0.8	0.5–0.7	0.22–0.56	0.39
Single/low-rise industrial buildings		1	1	0.8–0.9	0.8–0.9	0.85

Assessment of Photos

According to the layout characteristics of general urban buildings, each block area can be divided into two layout modes, multi-block layout and single-family/tower layout, to simplify the complex changes in urban building forms, as shown in Figure 4. Among them, the former is applicable to the general land use properties such as low multi-story/small high-rise buildings with an average building level (F) below 10, while the latter is applicable to land use properties of individual buildings such as commercial buildings, wholesale markets, and high-rise tower layouts with an average building level (F) above 10.

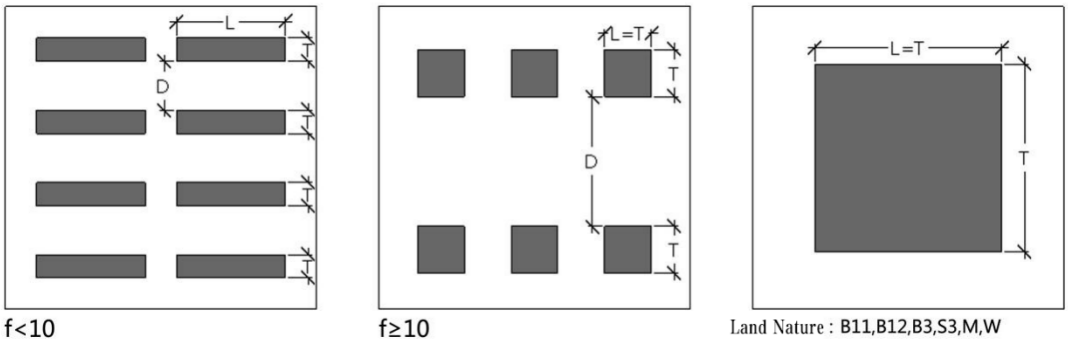

Figure 4. Simplified urban plot layout: Multi-block layout (**left**), tower layout (**middle**), single-family layout (**right**). Source: Drawn by the author.

The azimuth angle of the layout of each block is oriented towards the south to ensure that the south facade can receive maximum solar radiation. When each block has the same land use property, if multiple buildings are arranged in a row, each building has the same building depth (T). For energy conservation, single-family/tower layout buildings have the same building depth (T) and face width (L) to minimize their building size factor [30]. The values of general depth (T) and height (H) of reference buildings are determined from relevant codes, design regulations, and design experience values (Table 3). The area of the south facade of each block in the city can be roughly and statistically evaluated using Equations (10) and (11).

Table 3. In this paper, the depth (T) and height (h) of each type of building are taken from [31–33].

Nature of Land Use	Site Code	Floor Height h (m) Average	Depth of Entry T (m)
Administrative office land	A1	3.9	16
Cultural facilities land	A2	4.2	16
Educational and research land	A3	3.9	18
Primary school land	A33	3	10
Medical and health land	A5	3	24
Social welfare land	A6	3.6	16
Retail commercial land	B11	4.5	Single building layout T = L
Mixed commercial/hotel land	B11/B14	3.9	20
Mixed commercial/office land	B11/B2	3.9	16
Wholesale market land	B12	4.5	Single building layout T = L
Hotel land	B14	3.9	20
Business office land	B2	3.9	16
Recreation and sports land	B3	4.5	Single building layout T = L
Public utility business land	B4	3.9	18
Other service facilities land	B9	3.9	18
Industrial land	M1	6	Single building layout T = L
Residential land	R	3	15
Residential/commercial land	R/B11	3.2	15
Comprehensive transportation hub land	S3	4.5	Single building layout T = L
Storage and logistics land	W	6	Single building layout T = L

Statistics for the area of the south facade of multiple townhouses are calculated as follows:

$$Sn = f \cdot h \cdot \frac{Ar}{T} \quad (10)$$

Statistics for the area of the south facade of a single-family/tower layout are calculated as follows:

$$Sn = f \cdot h \cdot \sqrt{Ar} \quad (11)$$

Sn (m^2) is the statistical value of the south elevation area of a block. f is the number of proposed building floors for a certain block. h (m) is the general building height selected

according to the nature of land. Ar (m^2) is the roof area/floor area. T (m) is the general building depth selected according to the nature of land use.

Describe the window reduction coefficient (Kf) of the facade and the shadow reduction coefficient (Ks) of the facade. That is, the photovoltaic available area (Sf) of the south facade of each block can be expressed as follows:

$$Sf = Sn \cdot Kf \cdot Ks \tag{12}$$

For the value of Kf, we ignored the influence of shadow occlusion caused by the changes in the concave and convex shape of building facades, such as shading and projection, and calculated it only with the area ratio of window to wall (100%—window–wall area ratio). In combination with relevant codes [34], the value of Kf can be set as 0.55 for general buildings and as 1 for commercial buildings (B11). However, for general commercial building plots (B11) or mixed plots including commercial functions (B11/B14, B11/B2, R/B11), the first 1–2 floors of commercial building parts are usually not suitable for photovoltaic module installation due to their extremely high commercial value and should be excluded in the assessment of photovoltaic available facade area. In other words, the value of the proposed building floor (F) in each commercial and mixed parcel containing commerce in Equations (10) and (11) shall be considered by subtracting 1–2 floors.

As for the value of Ks, according to the standard, the sunshine duration of 6 h during the winter solstice should be guaranteed [35]. Therefore, in this paper, the elevation shadow reduction coefficient (Ks) of the multi-block layout was calculated at the most unfavorable time point (9:00 a.m. on the winter solstice). As shown in Figure 5, the ratio of photovoltaic available facade area to facade area (Ks) can be expressed as AB/AC and can also be expressed as C′c/C′o, according to the similar triangle theorem. The detailed calculation process is shown in Equations (13)–(16).

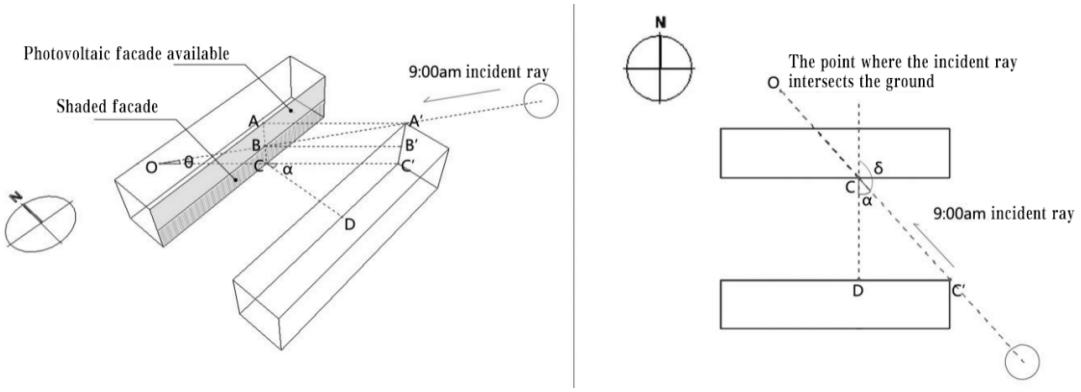

Figure 5. Calculation of the shadow reduction coefficient Ks of the multi-block layout facade. Source: Drawn by the author.

The Ks calculation process of multi-building row layout is determined as follows [35]:

$$Ks = \frac{AB}{AC} = \frac{A'B'}{A'C'} = \frac{B'B}{C'O} = \frac{C'C}{C'O} \tag{13}$$

$$C'C = \frac{CD}{\cos(180^\circ - \delta)} = \frac{L0 \cdot h \cdot f}{\cos(180^\circ - \delta)} \tag{14}$$

$$C'O = \frac{A'C'}{\tan\theta} = \frac{h \cdot f}{\tan\theta} \tag{15}$$

By substituting Equations (14) and (15) into Equation (13), we can get the following:

$$Ks = \frac{L0 \cdot \tan\theta}{\cos(180^\circ - \delta)} \tag{16}$$

Ks is the shadow reduction coefficient of the south-central facade of a multi-block layout. L0 is the reference sunshine spacing coefficient. h (m) is the general building height selected according to the nature of the land. f is the number of proposed building floors. δ means the azimuth angle of the sun at a certain time. θ is the height angle of the sun at a certain time.

At the same time, it is known that the sunshine spacing coefficient (L0) of Hohhot City is 1.73 (2 h on a major cold day) [36], the sun azimuth angle (δ) is 138.19° at 9:00 a.m. on the winter solstice, and the sun altitude angle (θ) is 13.34° (calculated according to the method in the literature [37]). By substituting Equations (5)–(15), we can calculate that the value of the facade shadow reduction coefficient (Ks) for the multi-building row layout in Hohhot is 0.55.

Assessment of Photovoltaic Available Area of a Parking Lot Surface

Approximately 10% of the land area of the parking lot and 20% of the canopy area cannot be utilized for photovoltaic installation. Finally, the available photovoltaic area of various parking lots can be expressed by Equation (17). The calculation results are shown in Figure 6.

$$St = 0.72 \cdot A \cdot P \quad (17)$$

St (m^2) is photovoltaic available area of a parking lot. P is the rate of ground parking land, assuming that the social parking lot and bus station are 100%.

Figure 6. Total available PV area of various blocks in Hohhot (roof, south facade, and ground parking area). Source: Drawn by the author.

2.2.5. Evaluation of Hourly Photovoltaic Power Generation

Under the condition that the available PV area of each block in the city is known, we can evaluate and calculate the hourly electricity production of each area. Considering the feasibility of urban distributed photovoltaic installations in the future, this paper selects a relatively common and cost-effective polysilicon solar cell module (with an average photoelectric conversion efficiency of about 16%) for calculation. It is also assumed that the roofs, facades, and ground parking areas of block buildings around the city are all installed with a relatively common tilt, and photovoltaic applications are carried out in a south-facing arrangement. The optimal tilt angle (β) of a photovoltaic installation is 37.78° (latitude 40.78° for Hohhot) according to the relevant provisions of the grid connection

system. This is calculated by subtracting 3 from the local latitude, as specified in the design specification of a photovoltaic power station.

In terms of statistical capacity per unit area (Cp) [38], we consulted the relevant specification for horizontal photovoltaic installations (roofs, various ground parking areas) and photovoltaic facade installations. We selected two distinct points in time during the year that represent the most unfavorable conditions to assess the spacing of photovoltaic modules, photovoltaic coverage, and capacity per unit area for each installation type.

The statistics of installed capacity per unit area can be calculated by determining the ratio between the projected area of PV modules and the available area of PV, that is, the PV coverage rate (Pr). This paper briefly describes the indicator as the ratio between the PV module projection length and the PV array spacing, as illustrated in Figures 7 and 8. The PV coverage of the horizontal plane and elevation can be calculated by referring to Equations (13)–(16). After substituting the local parameters in Hohhot, (at 9:00 on the winter solstice, the sun's altitude angle $\theta = 13.34^\circ$ and the sun's azimuth angle $\delta = 138.19^\circ$; at 12:00 on the summer solstice, the solar altitude angle $\theta = 72.62^\circ$, and the solar azimuth angle $\delta = 180^\circ$), it can be determined that the photovoltaic coverage rate of the horizontal plane is 75.4% and the photovoltaic coverage rate of the facade is 19.5%. According to Equations (18) and (19), the installed capacity per unit area of the horizontal plane (Cph) in Hohhot is 158 W/m^2, and the installed capacity per unit area of the facade (Cpv) is 53 W/m^2.

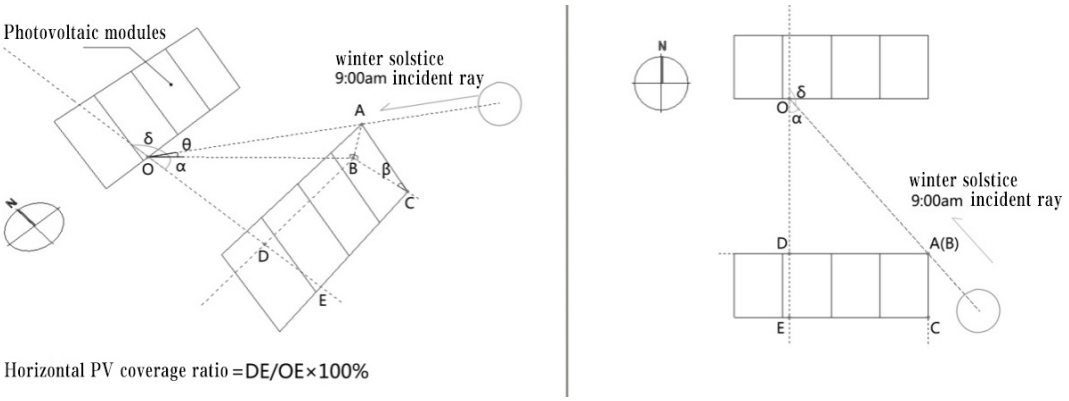

Figure 7. Calculation of the PV coverage when installed on an inclined horizontal plane. Source: Drawn by the author.

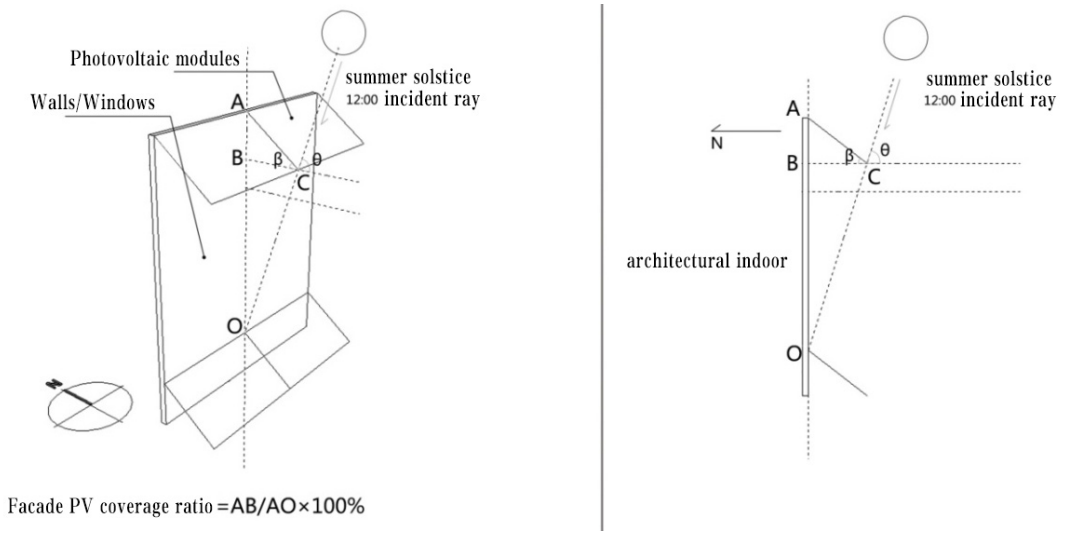

Figure 8. Calculation of the PV coverage when installed on a tilted facade. Source: Drawn by the author.

The installed capacity per unit area of the horizontal plane is as follows [35]:

$$Cph = \frac{Pw \cdot Pr}{Ap \cdot \cos\beta} \quad (18)$$

The installed capacity per unit area of facade plane is determined by the following:

$$Cpv = \frac{Pw \cdot Pr}{Ap \cdot \sin\beta} \quad (19)$$

Cph (W/m^2) is the estimated installed capacity per unit area of the horizontal plane of the proposed area. Cpv (W/m^2) is the estimated installed capacity per unit area of the proposed area facade. Pw (Wp) means the peak power (rated power) of the selected PV module. Pr is the PV coverage rate of the PV module installation area. Ap (m^2) is the area of the selected PV module. β is the best angle selected for photovoltaic module installation (37.78° in Hohhot).

3. Results and Discussion

3.1. Hourly Electricity Generation Calculation

After determining the installed capacity per unit area of the horizontal plane and facade, we can proceed to calculate the hourly power generation per unit area of photovoltaic panels. Firstly, the hourly meteorological forecast data for Hohhot City from 0:00 on 1 January 2019 to 23:00 on 31 December 2019 was selected from EnergyPlus. Then, we combined the SAM (System Advisor Model) PV Model analysis software (2015.1.30) provided by the United States National Renewable Energy Laboratory (NREL) to analyze the variation in hourly PV output power per unit area on the horizontal plane and facade in Hohhot city throughout the year (Figure 9).

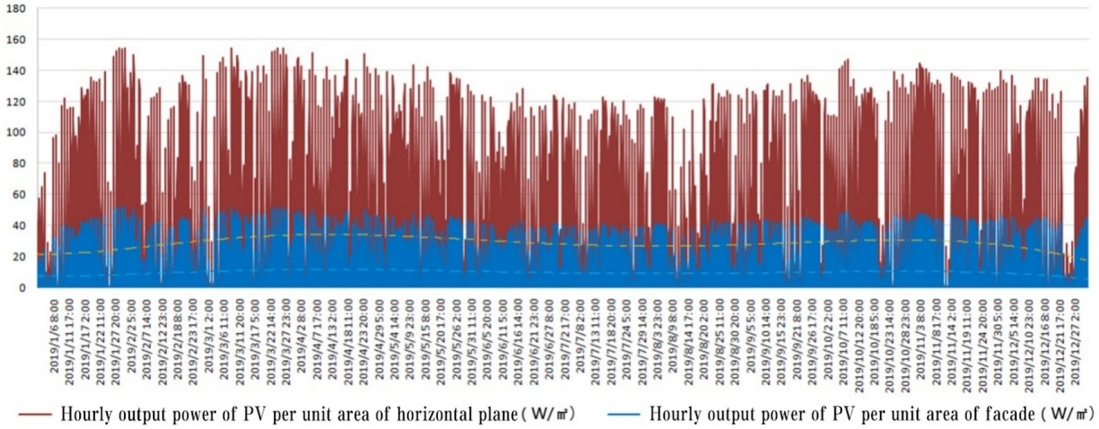

Figure 9. Annual hourly PV output per unit area of horizontal plane and facade of Hohhot. Source: exported by the author according to the analysis result of SAM.

The results indicate that the overall variation throughout the year remains stable, with a slight increase in photovoltaic electricity production observed during the periods from March to May and September to November. By utilizing SPSS software (26.0), we conducted k-means cluster analysis on the hourly PV output per unit area of Hohhot City throughout the year on a daily basis. This analysis helped us categorize the days with similar characteristics in terms of hourly PV output fluctuations. With this clustering (K = 10), we obtained a 10-category clustering result (as shown in Figure 10, arranged in descending order of occurrence days).

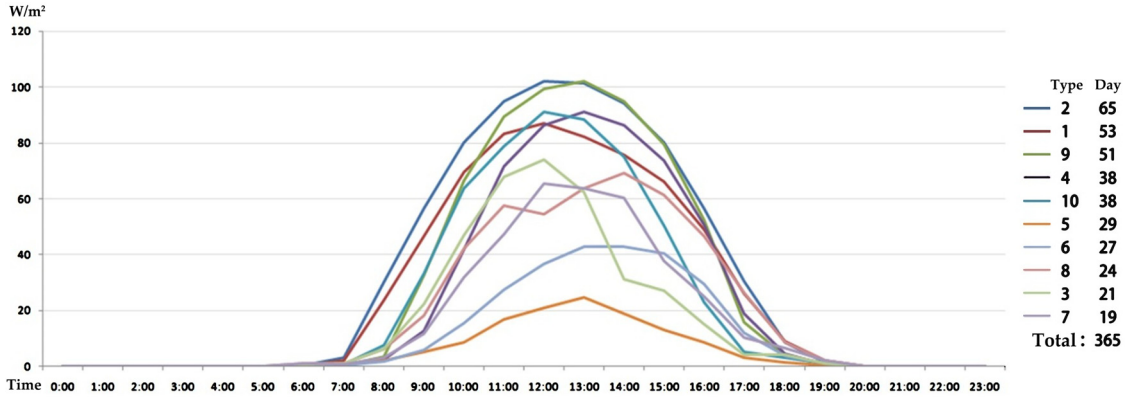

Figure 10. Classification results of annual hourly photovoltaic output changes per unit area of horizontal plane (clustering center). Source: Drawn by the author.

Categories 5, 6, 8, 3, and 7 are heavily affected by weather factors such as overcast rain, and their hourly photovoltaic power generation decreases in different periods. On the other hand, categories 2, 1, 9, 4, and 10 represent typical hourly photovoltaic power generation conditions on sunny days, with power generation being less affected by the weather. The average value of PV power output per unit area at each time point of these five types of curves is used as the standard hourly PV power output per unit area per day curve developed in this paper to reflect the local situation throughout the year (refer to Figure 11 for the results). Then, based on the installed capacity per unit area and the available PV area of the roof, facade, and ground parking area of each block, the total installed PV capacity, the total hourly PV power generation, and the hourly PV power generation density of each block can be calculated, as shown in Equations (20)–(22).

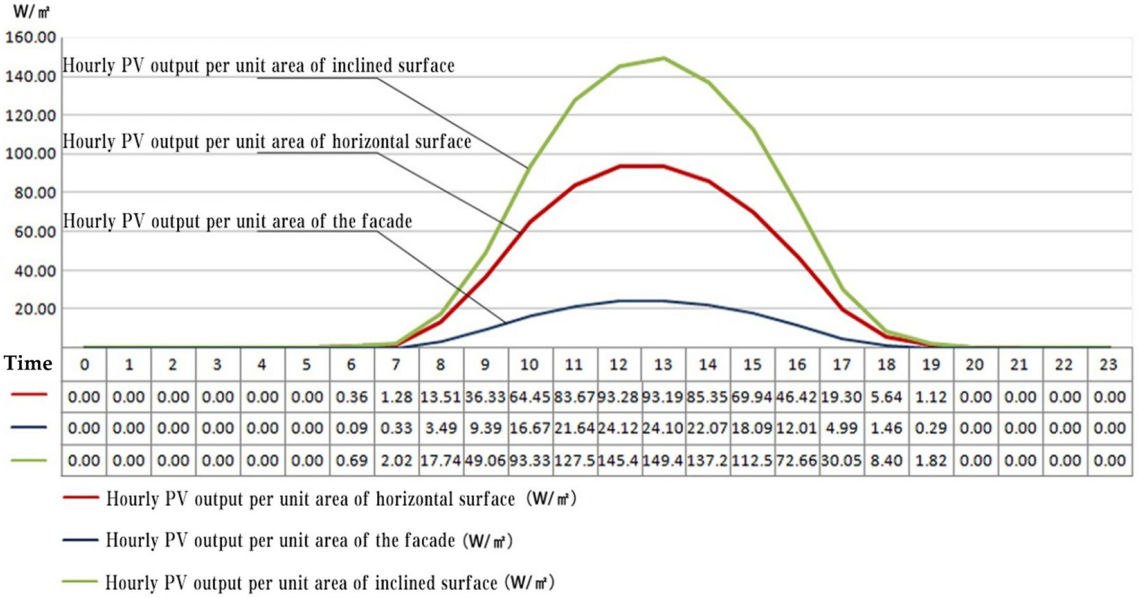

Time	0	1	2	3	4	5	6	7	8	9	10	11	12	13	14	15	16	17	18	19	20	21	22	23
	0.00	0.00	0.00	0.00	0.00	0.00	0.36	1.28	13.51	36.33	64.45	83.67	93.28	93.19	85.35	69.94	46.42	19.30	5.64	1.12	0.00	0.00	0.00	0.00
	0.00	0.00	0.00	0.00	0.00	0.00	0.09	0.33	3.49	9.39	16.67	21.64	24.12	24.10	22.07	18.09	12.01	4.99	1.46	0.29	0.00	0.00	0.00	0.00
	0.00	0.00	0.00	0.00	0.00	0.00	0.69	2.02	17.74	49.06	93.33	127.5	145.4	149.4	137.2	112.5	72.66	30.05	8.40	1.82	0.00	0.00	0.00	0.00

Figure 11. Hourly output power curve of standard daily PV per unit area used in this paper. Source: Drawn by the author.

The assessment of total installed PV capacity of each block is performed as follows:

$$C = Sr \cdot Cph + Sf \cdot Cpv + St \cdot Cph \quad (20)$$

The assessment of hourly photovoltaic power generation in various blocks is performed as follows:

$$PV_i = \frac{Sr \cdot Oph_i + Sf \cdot Opv_i + St \cdot Oph_i}{1000} \quad (21)$$

The assessment of hourly photovoltaic power generation density in various blocks is performed as follows:

$$PVd_i = \frac{1000 \cdot PV_i}{A} \quad (22)$$

C (W) is the total installed photovoltaic capacity of a certain block. Cph (W/m^2) is the estimated installed capacity per unit area of the horizontal plane of the proposed area. Cpv (W/m^2) is the estimated installed capacity per unit area of the proposed area façade.

Sr (m^2) is the available rooftop photovoltaic area. Sf (m^2) is the photovoltaic available area for a block building facade (south). St (m^2) is the photovoltaic available area of a block of ground parking area. PV_i (kWh) is the photovoltaic power generation of a certain area at the ith moment. Oph_i (W/m^2) is the photovoltaic output power per unit area of the horizontal plane at the ith time. Opv_i (W/m^2) is the photovoltaic output power per unit area of the facade at the ith time. PVd_i (Wh/m^2) is the photovoltaic power generation density at the ith moment.

3.2. Hourly Electricity Load Calculation

3.2.1. Load Density Index Method

In this paper, the power load forecasting method recommended in the Urban Power Planning Code [39], known as the load density index method (also referred to as the power per unit area method), is utilized to depict the electricity consumption of different buildings in the city. According to a survey conducted in cities of various sizes, focusing on urban planning and development, population planning, and the growth of residents' income levels, this method utilizes the general peak load power per unit area (W/m^2 or kW/km^2), known as the load density index [40], to assess the urban load level. This provides a reference for the power supply capacity configuration in this area. At the same time, since this method directly reflects the power load situation by the product of the building area or regional occupation area and load density index (Equation (23)), it is easier to effectively combine with the GIS geographic information system in terms of operation. This allows for a quick realization of the assessment of power load for various urban buildings.

In order to conduct hourly load assessments of different buildings in the city, this paper introduces the concept of hourly load rate (Lr_i) and the daily hourly load rate curve, drawing on the idea of power grid load rate. This approach aims to illustrate the variations in hourly load magnitude across different buildings. Finally, this paper provides a brief evaluation of the hourly power load of blocks in Hohhot City using two indices: load density and hourly load rate, as shown in Equation (24).

$$P_C = Ld \cdot A_{built} = Ld \cdot FAR \cdot A \quad (23)$$

$$Load_i = Lr_i \cdot Ld \cdot A_{built} \quad (24)$$

P_C (kW) is the peak load power (active power) of each building. Ld (W/m^2) is the load density of each building. A_{built} (m^2) is the building area. FAR is the floor area ratio of each block. A (m^2) is the land area of a certain place. $Load_i$ (kWh) is the power load at the ith moment of each block. Lr_i is the load rate at the ith moment of each block.

3.2.2. Load Density Index

The load density index is typically utilized to predict the power supply capacity configuration of different blocks, and its value also indicates the peak load of a block. In this paper, the proposed values of the load density index for various land uses are shown in Table 4.

Table 4. Partial land load density indicators selected in this paper [41–43].

Nature of the Land	Coding	Average Load Density <Ld> (W/m^2)	Simultaneous Factor (Kt)	Demand Factor (Kd)	Proposed Load Density Ld (W/m^2)
Residential land	R	55.00	0.95	0.43	22.09
Public administration and public service	A	74.44	0.98	0.75	54.44
Retail commercial land	B11	96.00	0.98	0.85	79.56
Wholesale market land	B12	62.50	0.98	0.85	51.80
Land for catering industry	B13	100.00	0.98	0.85	82.88
Land for the hotel	B14	70.00	0.98	0.85	58.01
Commercial office land	B2	81.00	0.98	0.85	67.13
Category I industry	M1	53.71	0.97	0.35	18.24
Category II industry	M2	59.43	0.97	0.38	21.62
Category III Industry	M3	74.00	0.97	0.43	30.51
Logistics and storage land	W	24.60	0.95	0.38	8.76
Municipal utility facilities	U	42.20	0.95	0.38	15.03
Green land and square land	G	2.00	0.95	0.75	1.43

Data Source: collated and calculated by the author according to relevant literature.

3.2.3. Daily Hourly Load Rate Curve

Analyzing the electricity load curves of various sections provided by Hohhot National Grid, we utilized SPSS software to classify the daily hourly load rate curves of 290 land samples based on the land use characteristics. Subsequently, we analyzed the clustering results to extract the most representative daily load rate curves of different land use types. These representative curves were then considered the typical daily load rate curves proposed in this paper (Figure 12).

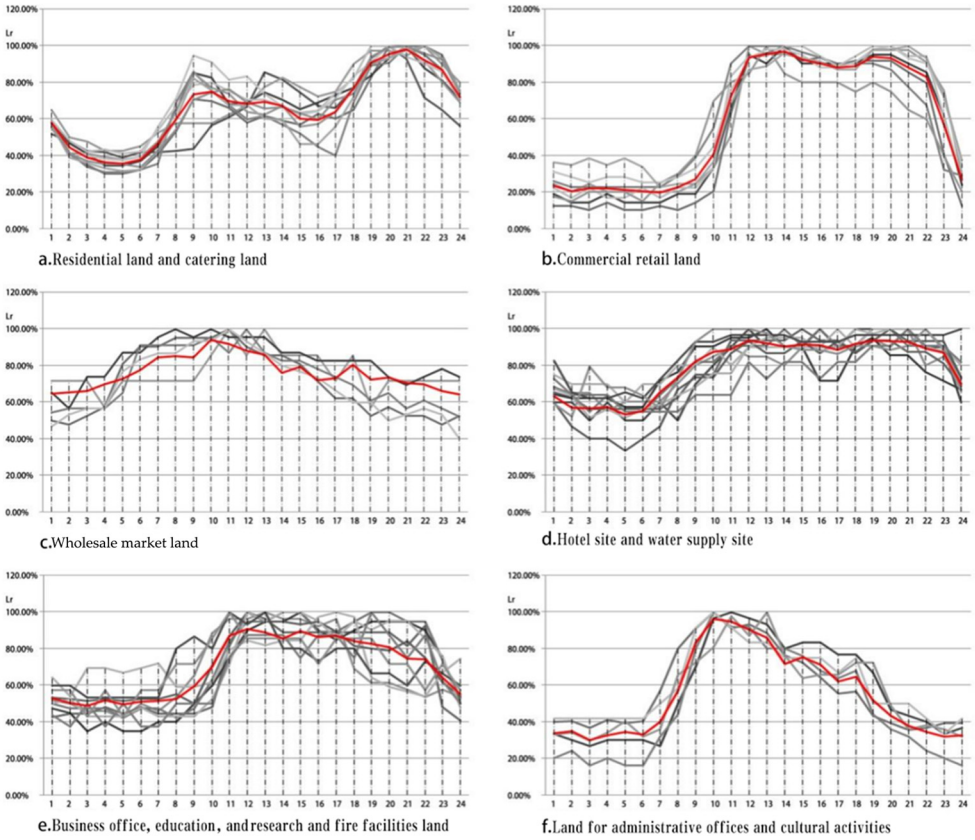

Figure 12. *Cont.*

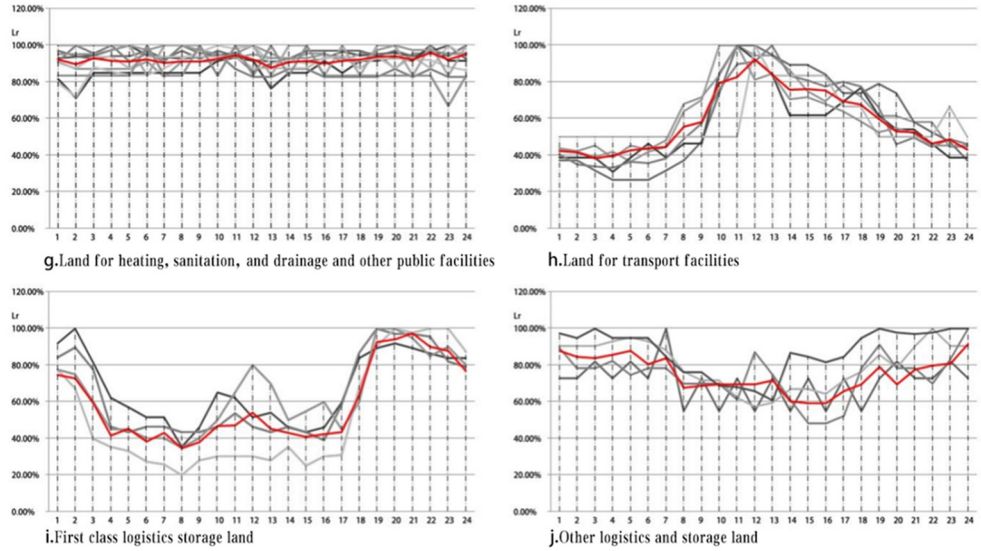

Figure 12. Daily load rate curve of each civil building block proposed in this paper (red): (**a**) Residential land and catering land; (**b**) Commercial retail land; (**c**) Wholesale market land; (**d**) Hotel site and water supply site; (**e**) Business office, education, and research and fire facilities land; (**f**) Land for administrative offices and cultural activities; (**g**) Land for heating, sanitation, and drainage and other public facilities; (**h**) Land for transport facilities; (**i**) First class logistics storage land; (**j**) Other logistics and storage land. Data source: Drawn by the author according to the results of SPSS cluster analysis.

3.2.4. Hourly Load Assessment for Mixed-Function Plots

In addition to the properties of all kinds of single-function land use, there are also various mixed-use plots in the city. These plots do not have a dominant single building function; instead, they showcase a variety of building functions coexisting. The mixed-function plot mainly combines horizontal and comprehensive functions. On a smaller scale (single building), it is primarily a combination of vertical and temporal dimensions. On a block scale, all four hybrids can be achieved.

Therefore, this paper selected 12 mixed commercial and other functional plots in Hohhot City and analyzed the proportion of the floor area of their respective commercial parts (Figure 13). The results show that most businesses account for between 20% and 40%. In order to facilitate the assessment of potential, this paper adopts the proportion of 30% commercial buildings as the standardized metric for all mixed-use plots. This means that the ratio of commercial to other building functional areas is 3:7. The peak load density and hourly daily load rate of all mixed-use plots are then calculated based on this standard. The peak load density values are B11/R: 39.67 W/m^2, B11/B14: 61.47 W/m^2, B11/B2: 65.72 W/m^2.

It is important to note that this article has established an ideal standard curve for photovoltaic power generation, depicting the hourly output per unit area. The results are derived from a year-long simulation of photovoltaic hourly output over 365 days. The analysis includes the calculation of the similarity to the average output power over 245 days, specifically focusing on the period from 6 to 7 p.m. Therefore, in the three indicators of daytime photovoltaic replacement rate (ESRd), photovoltaic utilization rate (PUR), and standard deviation of hourly replacement rate (Stdev), this paper uses a 13-hour period as the standard for calculation. The hourly PV power generation of each block is calculated based on the assessment results of the available PV area of each block and the proposed hourly PV power output curve per unit area of the standard daily area (Figure 12). The hourly power load of each block is determined by the proposed curve of hourly load rate for each functional building and the proposed index of load density for each functional building (Table 4), which is calculated using Equation (24). Then, according to Equations (1)–(3), the three indicators of ESRd, PUR, and Stdev of each block can be calculated, as shown in Figures 14–16.

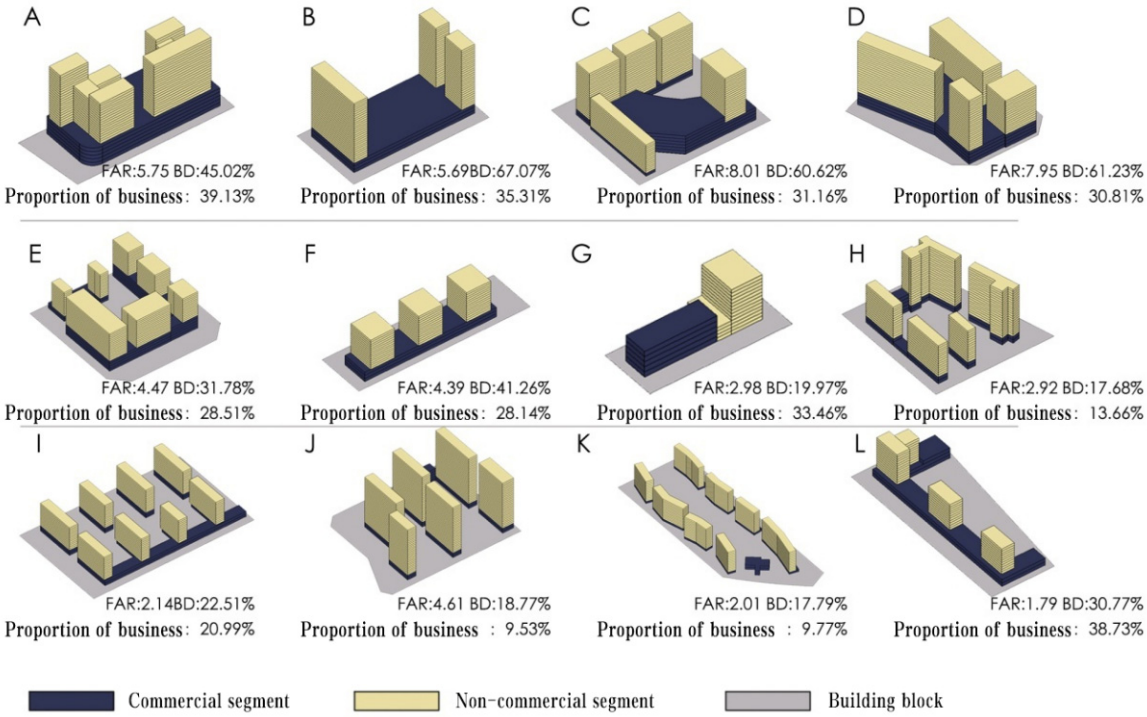

Figure 13. (**A**–**L**) Commercial area proportion of 12 commercial and other functional mixed plots selected in this paper: Source: Drawn by the author.

Figure 14. Daytime photovoltaic replacement rate (ESRd) of blocks in Hohhot.

Figure 15. Photovoltaic utilization rate of various blocks in Hohhot (PUR).

Figure 16. Standard deviation of inter-day displacement rate (Stdev) of blocks in Hohhot.

From the perspective of PV installation potential, the total area of suitable land for PV installation in all types of construction land in Hohhot is 1898.18 million square meters, accounting for 57.6% of the total construction land area. The total available rooftop PV area is 604,447,647 square meters, with an installed capacity of 95,507,028 kW. The total available PV area on the south elevation is 249,144,454 square meters, with an installed capacity of 132,046 kW. The total available PV area in the ground parking area is 49,499,580 square meters, with a total installed PV capacity of 78,203,034 kW. The total installed PV capacity in the city is about 10,464 MW. According to the typical daily hourly PV power generation, the theoretical average daily power generation can reach 44,015,000 kWh when tilt installation is adopted, accounting for approximately 73.7% of the daily electricity consumption of the entire society.

In terms of total photovoltaic power generation, Hohhot city presents optimistic development prospects due to its excellent solar radiation resources. In this paper, the average daytime PV replacement rate for all types of industrial sites is 82.9%, based on the daytime PV replacement rate (ESRd). This reflects the application of PV to replace traditional energy sources during off-peak production periods in all types of plants, even when there is excess power output. After considering the hourly electricity usage per unit of land for PV generation, the actual daily shipments in the city amount to 31,281 million kWh, representing approximately 52.4% of the total electricity consumption (citywide PV replacement rate). In other words, around 28.9% of the PV generation is theoretically wasted due to mis-match with the electricity load, which is equivalent to an indirect loss of 12,734 million kWh of electricity output per day.

The stability of hourly photovoltaic power supply is determined by the standard deviation of the hourly photovoltaic replacement rate (Stdev). Spatial quantification of photovoltaic energy using urban data is becoming an important element of future smart cities and sustainable development. On the whole, the average Stdev of the city is 23.8%, which indicates relative stability in terms of the overall variability within the city. The average Stdev level of all types of industrial land is the highest at 38.9%, indicating significant instability. Residential and office space occupancy rates are relatively stable at 21.8% and 15.9%, respectively. The most stable type of land is commercial land, with an average Stdev of 8.8%. The main reason is that the land has a high load density, and the impact of photovoltaic power is not significant. Even after the implementation of photovoltaic systems, urban distribution networks still need to maintain a high level of capacity allocation and power supply to ensure reliable electricity distribution.

3.3. Cluster Analysis of Power Characteristic Laws of Different Plots

In order to summarize the evolving patterns of daily power characteristics following the implementation of PV power generation at various sites, this study conducted a cluster analysis of 5023 plots in the city using three indicators: daytime PV replacement rate, PV utilization rate, and PV utilization stability (Table 5). Additionally, a regression analysis was carried out to examine the relationship between each indicator and the floor area ratio (FAR) (Figure 17).

Table 5. Cluster analysis of daily power characteristics after PV installation.

Category	Center of Clustering			Major Building Features and Their Corresponding Floor Area Ratio Ranges
	ESRd/%	PUR/%	Stdev/%	
1	0.00	0.00	0.00	Cultural relics, monuments, religious facilities, special sites, various types of plazas, green spaces, water bodies, and other areas where photovoltaic installation is not feasible
2	88.52	1.20	24.79	Various types of social car parks
3	79.67	5.12	37.01	Primary and secondary schools (0.8–1.19), logistics warehouses (0.8)
4	79.25	11.43	40.27	Executive offices (0.8–0.99), primary and secondary schools (1.2–2.2), various industrial buildings (0.8), integrated traffic hubs (0.86–1.49)
5	52.32	26.58	40.55	Executive offices (1.11–2.13), educational research (0.84–2.1), medical and health (0.81–1.47), residences (0.85–1.78), mixed residential/commercial (0.82–1.04), integrated traffic hubs (1.71–2.58)
6	29.31	28.66	25.70	Executive offices (2.19–3.21), educational research (2.12–3.82), medical and health (2.22–3.57), commerce (0.96–1.31), mixed commercial/offices (0.97–1.29), business offices (0.83–1.18), residences (1.82–2.94), mixed residential/commercial (1.44–1.84)
7	19.18	28.25	15.67	Executive offices (3.53–4.33), educational research (3.8–4.15), medical and health (3.65–4.38), commerce (1.42–1.76), mixed commercial/offices (1.34–2.32), business offices (1.2–2.1), residences (2.95–4.39), mixed residential/commercial (1.89–3.4)
8	10.73	28.80	7.59	Executive offices (5.92–5.98), educational research (4.24–4.38), commerce (1.93–3.8), mixed commercial/hotels (2.53–5.74), mixed commercial/offices (2.34–6.0), business offices (2.19–5.64), residences (5.74–5.94), mixed residential/commercial (3.32–5.81)

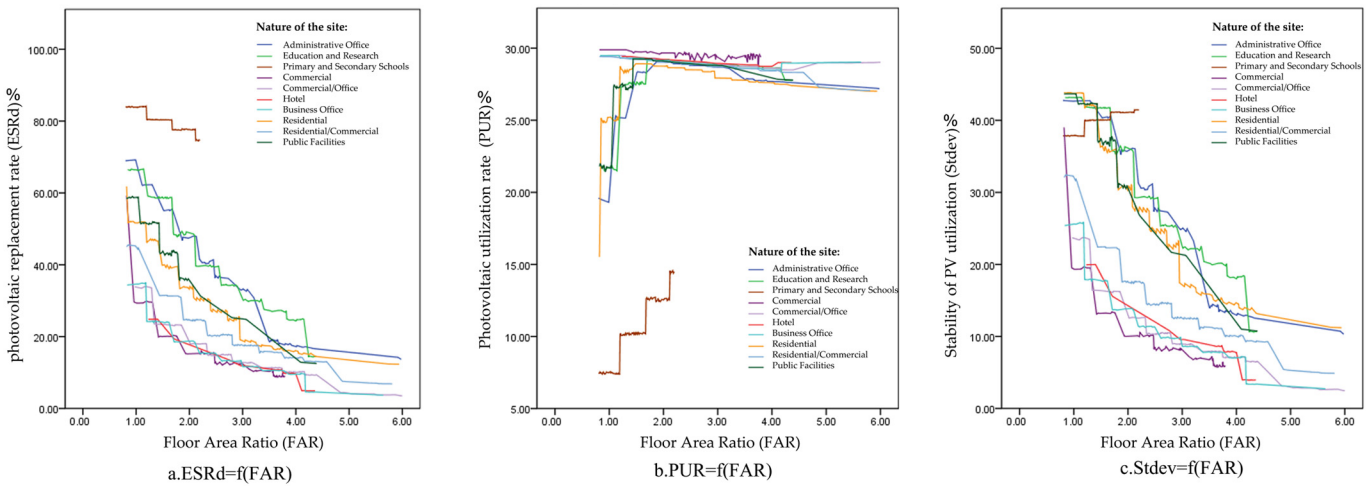

Figure 17. Regression analysis of ESRd = f(FAR), PUR = f(FAR), Stdev = f(FAR).

After considering the time sequence of PV power consumption, all urban land plots can be categorized into three main types: PV unsuitable land plots (category 1), PV excess power land plots (categories 2 to 4), and general PV application land plots (categories 5 to 8). Among them, the areas with excess PV power mainly include industrial areas, warehouses, car parks, primary and secondary schools, and other building plots with insufficient power consumption. The replacement rate of PV systems is excessively high, and the surplus

power cannot be consumed during the peak hours of PV power generation. As a result, the PV utilization rate is very low, and the replacement rate fluctuates significantly throughout the day (categories 3 and 4). The general PV application areas mainly include commercial, office, residential, and other civil buildings. Based on the results of the evaluation and analysis (Table 5, Figure 17), it is evident that the variation in electricity load demand due to differences in plot ratio will significantly influence the electricity consumption patterns following the installation of photovoltaic systems in each plot. Therefore, it is of great significance to enhance the overall PV potential of the city by effectively controlling the planning layout and plot ratio of each site.

As far as the stage of PV development is concerned, traditional fossil energy generation, mainly thermal power, will continue to dominate as a reliable energy source for an extended period. However, the current thermal turbines are generally characterized by slow start-up and shutdown, high minimum technical output requirements, lack of flexibility in system regulation, and rigidity in power scheduling. These limitations may pose challenges in meeting the future demands of renewable energy development. Considering its development goals, this paper takes the 40% daytime PV replacement rate as the best criterion to measure the proportion of PV power consumption in each urban area. During the daytime when PV energy is available, 40% of the load demand is supplied by PV in combination with a small amount of energy storage to ensure voltage stability. The remaining load demand is met by 40% of the minimum thermal power output and 20% from other renewable energy sources. As can be seen in Table 4, the daytime PV replacement rate in the areas of plot 5 and plot 6 has a better match with this criterion, with ESRd values of 52.32% and 29.31%, respectively. Meanwhile, it can be seen from Figure 17 that under different plot ratios, there is a theoretical maximum peak value of the PV utilization rate for each plot. However, due to the relatively low plot ratio of category 5, its economic return from PV systems is poor. At the same time, the stability of the power supply also reflects a significant disadvantage, with a Stdev value as high as 40.55%. This high variability is relatively unfavorable for regulating the thermal system, given the substantial demand of the grid connection. After a comprehensive comparison, the building plot ratio interval for each type of building will serve as the standard for the sixth type of land, which will be more favorable to the overall PV potential of Hohhot. The corresponding values of the functional plot ratios for each type of building in this category will become the primary focus for adjusting urban planning in the future. It can be further seen that various types of small high-rise (average number of floors 6–9) building forms in the city may be better suited to meet the needs of urban PV utilization and will likely become the primary spatial layout for future urban development. These building forms include residential buildings, administrative office buildings, and more.

In addition, as shown in Table 5, the PV replacement rate is high for all types of industrial land (Class 3 and 4) in the city, indicating a clear surplus of electricity output. The paper examines the impact of the demand coefficient, which indicates that not all power equipment is activated simultaneously. The power load is only represented by daily office, lighting, and other non-production loads. In fact, various types of industrial buildings require significant power loads during peak production hours. Typically, these power needs are met by specific power plants through dedicated lines to ensure a consistent power supply. However, photovoltaic power faces challenges in meeting these demands due to its inherent instability and intermittency characteristics. Hence, industrial plants situated far from other urban functions and centrally located in isolated patches may experience minimal actual benefits from PV applications.

In addition, due to the higher load density in commercial, hotel, business office, and other land areas in the city (categories 7, 8), the overall rate of photovoltaic replacement is low. According to this paper, various types of building functions need to adjust the volume ratio interval. The average volume ratio needs to be adjusted downward to 0.96–1.31 (for instance, in commercial buildings, the average number of floors is typically 2–3). Otherwise, the shape of the building will exceed the reasonable design range and be challenging to

realize. Therefore, it is difficult to realize the future urban development of the above area. Therefore, for future adjustments to urban planning in the aforementioned areas, more consideration should be given to facilitating the layout of neighborhoods or even the organic integration of these areas while ensuring that the normal operation of the city is not disrupted.

4. Conclusions

The strategic deployment of installed PV systems within built environments is paramount for driving future urban renewable energy structural transformations. Simply focusing on guiding PV planning and construction based on total power generation at a singular level cannot fully exploit the potential benefits of this approach. The urban distributed photovoltaic energy evaluation model introduced in this paper offers a more comprehensive integration of future energy needs with sustainable urban development. It lays the groundwork for incorporating Internet of Things and big data technologies, which are crucial for maximizing future urban energy potential. However, as this paper solely addresses the optimization of PV potential in Hohhot city concerning a single spatial layout issue of volume ratio adjustment, several limitations remain regarding parameter selection, data accuracy, and influencing factors. Future research should encompass a broader spectrum of practical social development issues, such as economic growth, urban planning, and industrial adaptations. This holistic approach will facilitate strategic planning of urban energy spatial layouts, fostering the transformation of photovoltaic power energy structures and advancing sustainable urbanization.

Author Contributions: Conceptualization, Z.Z.; methodology, S.C. and C.W.; software, S.C.; validation, L.T., H.L. and R.H.; date analysis, S.C. and Z.Z.; investigation, S.C. and C.W.; resources, S.C. and R.Z.; data curation, H.L. and H.Y.; writing-original draft preparation, S.C.; writing-review and editing, H.L., H.Y. and R.H.; visualization, Z.Z. and R.H.; supervision, C.W., H.Y. and R.Z.; project administration, L.T.; funding acquisition, L.T. and R.Z. All authors have read and agreed to the published version of the manuscript.

Funding: This work was supported by the National Natural Science Foundation of China (52078324); the National Natural Science Foundation of China (52078322); Tianjin University Graduate Students' Award Program for Outstanding Innovation in Arts and Sciences (A1-2022-005) and Tianjin Graduate Student Research Innovation Program (2022BKY093).

Data Availability Statement: The raw data supporting the conclusions of this article will be made available by the authors on request.

Conflicts of Interest: Author Siyuan Chen was employed by the company China Northeast Architectural Design & Research Institude Co., Ltd. The remaining authors declare that the research was conducted in the absence of any commercial or financial relationships that could be construed as a potential conflict of interest.

Nomenclature

Ar (m^2)	Roof area/floor area
Ap (m^2)	Area of selected PV module
A_{built} (m^2)	Building area
β	Best angle (37.78° in Hohhot)
BD′	Building density
BD	Proposed building density
Cph (W/m^2)	Installed capacity per unit area of the horizontal plane
Cpv (W/m^2)	Installed capacity per unit area of the facade
C (W)	Installed photovoltaic capacity
ESR_i	Hourly Energy Substitution Rate
ESR	Overall Energy Substitution Rate
FAR	Floor area ratio

F'	Average number of building floors
F/f	Proposed number of building floors
G	Green land rate
H (m)	Building height
Kf	Window reduction coefficient
Ks	Facade and shadow reduction coefficient
Kr	Rooftop photovoltaic utilization coefficient
Ld (W/m^2)	Load density of each building
$Load_i$ (kWh)	Power load at the ith moment
Lr_i	Load rate at the ith moment
L0	Reference sunshine spacing coefficient
N	Number of power generation hours
Oph_i (W/m^2)	Photovoltaic output power per unit area of the horizontal plane at the ith time
Opv_i (W/m^2)	Photovoltaic output power per unit area of the facade at the ith time
PUR	Photovoltaic utilization rate
Pw (Wp)	Peak power (rated power)
Pr	PV coverage rate
PV_i (kWh)	Photovoltaic power generation at the ith moment
PVd_i (Wh/m^2)	Photovoltaic power generation density at the ith moment
Pc (kW)	Peak load power (active power)
P	Percentage of ground parking land
Pe_i (kWh)	Consumption of photovoltaic power
PV_i (kWh)	Photovoltaic power generation
R	Land use rate
R_i	Arithmetic average of daily hourly PV replacement rate
Stdev	Standard deviation of hourly PV replacement rate
Sr (m^2)	Available rooftop photovoltaic area
Sf (m^2)	Available area for photovoltaic of a block building facade (south)
St (m^2)	Photovoltaic available area of a block of ground parking area
Sn (m^2)	Statistical value of the south elevation area
Sf	Photovoltaic available area
S	Rate of supporting public construction land
T (m)	Building depth
δ	Sun azimuth

References

1. UN-Habitat. *World Cities Report 2020: The Value of Sustainable Urbanization*; United Nations Human Settlements Programme: Nairobi, Kenya, 2020.
2. Kartal, G. The Effects of Positive and Negative Shocks in Energy Security on Economic Growth: Evidence from Asymmetric Causality Analysis for Turkey. *Econ. Comput. Econ. Cybern. Stud. Res.* **2022**, *56*, 223–240.
3. Yoon, J.; Joung, S. Environmental self-identity and purchasing ecofriendly products. *J. Logist. Inform. Serv. Sci.* **2021**, *8*, 82–99.
4. IRENA. *Future of Solar Photovoltaic: Deployment, Investment, Technology, Grid Integration and Socio-Economic Aspects (A Global Energy Transformation: Paper)*; International Renewable Energy Agency: Abu Dhabi, United Arab Emirates, 2019.
5. Root, L.; Perez, R. *Photovoltaic Covered Parking Lots: A Survey of Deployable Space in the Hudson River Valley, New York City, and Long Island, New York*; Atmospheric Sciences Research Center: Albany, NY, USA, 2006.
6. Xiong, Y.; Liu, X.; Ma, S. Analysis on application conditions of urban scale photovoltaic power generation in China. *Renew. Energy Resour.* **2012**, *30*, 123–126.
7. Manni, M.; Formolli, M.; Boccalatte, A.; Croce, S.; Desthieux, G.; Hachem-Vermette, C.; Kanters, J.; Ménézo, C.; Snow, M.; Thebault, M.; et al. Ten questions concerning planning and design strategies for solar neighborhoods. *Build. Environ.* **2023**, *246*, 110946. [CrossRef]
8. IEA. *PVPS Task VII, Potential for Building Integrated Photovoltaics*; International Energy Agency: Paris, France, 2002.
9. Izquierdo, S.; Rodrigues, M.; Fueyo, N. A Method for Estimating the Geographical Distribution of the Available Roof Surface Area for Large-Scale Photovoltaic Energy-Potential Evaluations. *Sol. Energy* **2008**, *82*, 929–939. [CrossRef]
10. Jouri, K. *Planning for Solar Buildings in Urban Environments an Analysis of the Design Process, Methods and Tools*; Department of Architecture and Built Environment, Faculty of Engineering LTH, Lund University: Lund, Sweden, 2015.
11. Zhao, B.; Xiao, C.; Xu, C. Analysis of absorptive capacity of distributed photovoltaic grid connection in regional distribution network based on permeability. *Electr. Power Syst.* **2017**, *21*, 111–117.

12. Cheng, M.; Zhao, S.; Wu, L. Comprehensive evaluation of urban photovoltaic power generation projects based on AHP-TOPSIS. *Electr. Power* **2016**, *49*, 171–175.
13. Sigrid Lindner of Ecofys. Solar Urban Planning Berlin [EB/OL]. Available online: http://www.pvupscale.org/IMG/pdf/Berlin.pdf (accessed on 10 May 2020).
14. Zhang, H. *Study on the Evaluation of Photovoltaic Utilization Potential of Urban Building Roofs*; Tianjin University: Tianjin, China, 2017.
15. Enongene, K.E.; Abanda, E.H.; Otene, I.J.J.; Obi, S.I.; Okafor, C. The potential of solar photovoltaic systems for residential homes in Lagos city of Nigeria. *J. Environ. Manag.* **2019**, *244*, 247–256. [CrossRef] [PubMed]
16. Rosas-Flores, J.A.; Zenon-Olvera, E.; Galvez, D.M. Potential energy saving in urban and rural households of Mexico with solar photovoltaic system using geographical information system. *Renew. Sustain. Energy Rev.* **2019**, *116*, 109412. [CrossRef]
17. Bodis, K.; Kougias, I.; Jager-Waldau, A.; Taylor, N.; Szabo, S. A high-resolution geospatial assessment of the rooftop solar photovoltaic potential in the European Union. *Renew. Sustain. Energy Rev.* **2019**, *114*, 109309. [CrossRef]
18. Verso, A.; Martin, A.; Amador, J.; Dominguez, J. GIS-based method to evaluate the photovoltaic potential in the urban environments: The particular case of Miraflores de la Sierra. *Sol. Energy* **2015**, *117*, 236–245. [CrossRef]
19. Saadaoui, H.; Ghennioui, A.; Ikken, B.; Rhinane, H.; Maanan, M. Using GIS and photogrammetry for assessing solar photovoltaic potential on Flat Roofs in urban area case of the city of Ben Guerir/Morocco. In Proceedings of the 5th International Conference on Geoinformation Science—GeoAdvances 2018, Casablanca, Morocco, 10–11 October 2018; Copernicus Publications: Göttingen, Germany, 2019; Volume XLII-4/W12, pp. 155–166.
20. Wang, L.Z.; Tan, H.W.; Ji, L.; Wang, L. A method for evaluating photovoltaic potential in China based on GIS platform[C]//IOP Conference Series: Earth and Environmental Science. *IOP Publ.* **2017**, *93*, 012056.
21. Kozlovas, P.; Gudzius, S.; Ciurlionis, J.; Jonaitis, A.; Konstantinaviciute, I.; Bobinaite, V. Assessment of technical and economic potential of urban rooftop solar photovoltaic systems in Lithuania. *Energies* **2023**, *16*, 5410. [CrossRef]
22. Alhamwi, A.; Medjroubi, W.; Vogt, T.; Agert, C. Development of a GIS-based platform for the allocation and optimisation of distributed storage in urban energy systems. *Appl. Energy* **2019**, *251*, 113360. [CrossRef]
23. Tapia, M.; Ramos, L.; Heinemann, D.; Zondervan, E. Power to the city: Assessing the rooftop solar photovoltaic potential in multiple cities of Ecuador. *Phys. Sci. Rev.* **2023**, *8*, 2285–2319. [CrossRef]
24. Liu, J.; Wu, Q.; Lin, Z.; Shi, H.; Wen, S.; Wu, Q.; Zhang, J.; Peng, C. A novel approach for assessing rooftop-and-facade solar photovoltaic potential in rural areas using three-dimensional (3D) building models constructed with GIS. *Energy* **2023**, *282*, 128920. [CrossRef]
25. Bernasconi, D.; Guariso, G. Rooftop PV: Potential and Impacts in a Complex Territory. *Energies* **2021**, *14*, 3687. [CrossRef]
26. Fu, R.; Timothy, R.; Robert, M. *2018 U.S. Utility—Scale Photovoltaics-Plus-Energy Storage System Costs Benchmark*; National Renewable Energy Laboratory: Oak Ridge, TN, USA, 2018.
27. Inner Mongolia Hohhot Bureau of Statistics. *2023 Hohhot City Statistical Yearbook [EB]*; Hohhot Bureau of Statistics: Huhehaote, China, 2023.
28. Andson, K.; Coddington, M.; Burman, K. *Interconnecting PV on New York City's Secondary Network Distribution System*; National Renwable Energy Laboratory: Golden, MO, USA, 2009.
29. Hua, Z. *Research on the Assessment of the Potential of Urban Building Rooftop Photovoltaic Utilization*; Tianjin University: Tianjin, China, 2017.
30. Ren, B. *Research on Low Energy Consumption Design Prototype of Multi-Storey Office Buildings in Cold Regions*; Tianjin University: Tianjin, China, 2014.
31. Hang, Z. *Zhejiang Province of Planning Bureau, Rules for Building Storey Height Control and Floor Area Ratio Index Calculation*; Hangzhou Municipal Planning Bureau: Hangzhou, China, 2010.
32. *GB50099-2011*; Ministry of Housing and Urban-Rural Construction of the People's Republic of China. Code for Design of Primary and Secondary Schools. Guangming Daily Press: Beijing, China, 2011.
33. *GB 51039-2014*; National Health and Family Planning Commission of the People's Republic of China. Code for Design of Polyclinic Buildings. China Planning Press: Beijing, China, 2014.
34. *GB50189-2015*; China Academy of Building Sciences. Design Standard for Energy Efficiency of Public Buildings. China Building Industry Press: Beijing, China, 2015.
35. *GB50797-2012*; China Electricity Council. Code for Design of Photovoltaic Power Station. China Planning Press: Beijing, China, 2012.
36. *GB50180-93*; Ministry of Housing and Urban Rural Development of the People's Republic of China. Code for Planning and Design of Urban Residential Areas. China Building Industry Press: Beijing, China, 2002.
37. Brito, M.; Freitas, S.; Guimar, E. The importance of facades for the solar PV potential of a Mediterranean city using LiDAR data. *Renew. Energy* **2017**, *111*, 85–94. [CrossRef]
38. *JGJ203-2010*; Ministry of Housing and Urban Rural Development of the People's Republic of China. Technical Code for Application of Solar PV System in Civil Buildings. China Construction Industry Press: Beijing, China, 2010.
39. *GB/T50293-2014*; Ministry of Housing and Urban Rural Development of the People's Republic of China. Code for Urban Power Planning. China Construction Industry Press: Beijing, China, 2014.
40. The General Institute of Electric Power Planning and Design. *Ministry of Electric Power Industry, Power System Design Manual*; China Electric Power Press: Beijing, China, 1998.

41. China Institute of Building Standards Design. *Technical Measures for National Civil Building Engineering Design: 2009 Edition, Electrical*; China Planning Press: Beijing, China, 2009.
42. Ye, X. *Research on Power Load Index of Ningbo Unit Construction Land, Urban Times, Collaborative Planning—2013 China Urban Planning Annual Conference*; China Urban Planning Society: Beijing, China, 2013.
43. Liu, D.; Zhu, Y.; Zhang, Q. Discussion on the Value of Load Index, Demand Coefficient and Synchronization Coefficient in Urban Power Planning. *Archit. Eng. Technol. Des.* **2014**, *10*, 16.